Mechanochemical Synthesis of High Lithium Ion Conducting Materials in the System Li_3N-SiS_2

Keiichi Iio, Akitoshi Hayashi, Hideyuki Morimoto, Masahiro Tatsumisago,* and Tsutomu Minami

Department of Applied Materials Science, Graduate School of Engineering, Osaka Prefecture University, Sakai, Osaka 599-8531, Japan

Received August 22, 2001. Revised Manuscript Received March 13, 2002

High lithium ion conducting materials were mechanochemically synthesized using Li_3N and SiS_2 as starting materials. The obtained Li_3N-SiS_2 materials were almost amorphous; the amorphous phases consisted of SiS_4 tetrahedral units with no edge sharing and the local structure was very similar to that of mechanically milled Li_2S-SiS_2 amorphous materials. High lithium ion conducting Li_3N-SiS_2 materials could be synthesized in very short milling periods, around 20 min, since explosive reactions occurred in this system. The mechanically milled $40Li_3N{\cdot}60SiS_2$ (mol %) material exhibited excellent properties as solid electrolytes such as high conductivity around 10^{-4} S cm^{-1} at room temperature, unity of lithium ion transport number, and a wide electrochemical window of about 10 V vs Li^+/Li.

1. Introduction

Lithium ion secondary batteries with high capacities and high energy densities have been popularized since several portable electronic instruments such as cellular phones and notebook-type personal computers have been developed. A safety problem, however, has been noted for such batteries because they include flammable organic liquid electrolytes.[1] If nonflammable inorganic solid electrolytes could be used, their safety and reliability might be remarkably improved. Therefore, high lithium ion conducting inorganic solid electrolytes are required.

Lithium nitride (Li_3N) crystals attracted much attention as solid electrolytes because of their extremely high ion conductivity (1.2×10^{-3} S cm^{-1} at 25 °C).[2,3] However, it is difficult to use Li_3N itself as an electrolyte for lithium ion secondary batteries since the decomposition voltage of Li_3N is very low (0.445 V).[3] To overcome this problem, a variety of Li_3N-based systems have been studied.[4−8]

Sulfide glasses in the system Li_2S-SiS_2 are one of the most promising solid electrolytes.[9−11] The glasses exhibit high conductivities on the order of 10^{-4} S cm^{-1} at room temperature and high electrochemical stability in a wide potential range of 10 V. Recently, we prepared $Li_2S-SiS_2-Li_3N$ glasses by a melt-quenching technique using Li_3N as a nitrogen source as well as a lithium source.[12] The addition of Li_3N to the Li_2S-SiS_2 system increased both the glass transition temperature and the crystallization temperature because of an incorporation of nitrogen atoms into the sulfide glass network. The glasses also exhibited high electrochemical stability in a wide potential range of 10 V. However, amounts of incorporated nitrogen atoms into the glasses were much smaller than those of nominal ones probably because nitrogen atoms vaporized during the melting process.

On the other hand, much attention has been paid to a mechanical milling technique using a high-energy ball mill as one of the new preparation procedures for inorganic compounds and amorphous materials.[13−21] The mechanical treatment for a mixture brings about an increase in contact areas among reactants and a local increase in pressure and temperature at contact surfaces. Therefore, surfaces of the mixture are changed because of a distortion of crystal structure and a redistribution of point defects, and then chemical reactions occur on the contact surfaces.[13−19] These reactions

(1) Tobishima, S.; Takei, K.; Sakurai, Y.; Yamaki, J. *J. Power Sources* **2000**, *90*, 188.
(2) Rabenau, A. *Solid State Ionics* **1982**, *6*, 277.
(3) Bell, M. F.; Breitschwerdt, A.; von Alpen, O. *Mater. Res. Bull.* **1981**, *16*, 267.
(4) Obayashi, H.; Nagai, R.; Gotoh, A.; Mochizuki, S.; Kudo, T. *Mater. Res. Bull.* **1981**, *16*, 587.
(5) Hartwig, P.; Weppner, W.; Wichelhaus, W. *Mater. Res. Bull.* **1979**, *14*, 493.
(6) Lapp, T.; Skaarup, S.; Hooper, A. *Solid State Ionics* **1983**, *11*, 97.
(7) Yamane, H.; Kikkawa, S.; Horiuchi, H.; Koizumi, M. *J. Solid State Chem.* **1986**, 65.
(8) Yamane, H.; Kikkawa, S.; Koizumi, M. *Solid State Ionics* **1987**, *25*, 183.
(9) Pradel, A.; Ribes, M. *Solid State Ionics* **1986**, *18/19*, 351.
(10) Kennedy, J. H. *Mater. Chem. Phys.* **1989**, *23*, 29.
(11) Hayashi, A.; Araki, R.; Komiya, R.; Tadanaga, K.; Tatsumisago, M.; Minami, T. *Solid State Ionics* **1998**, *113−115*, 733.
(12) Sakamoto, R.; Tatsumisago, M.; Minami, T. *J. Phys. Chem.* **1999**, *103*, 4029.
(13) Boldyrev, V. V.; Avvakumov, E. G. *Russ. Chem. Rev.* **1971**, *10*, 40.
(14) Schwarz, R. B.; Koch, C. C. *Appl. Phys. Lett.* **1986**, *49*, 146.
(15) Politis, C.; Johnson, W. L. *J. Appl. Phys.* **1986**, *60*, 1147.
(16) Koch, C. C. *Scr. Mater.* **1996,** *34*, 21.
(17) Balaz, P.; Bastl, Z.; Brancin, J.; Ebert, I.; Lipka, J. *J. Mater. Sci.* **1992**, *27*, 653.
(18) Boldyrev, V. V. *Solid State Ionics* **1993**, *63−65*, 537.
(19) Balaz, P.; Balintova, M.; Bastl, Z.; Brancin, J.; Sepelak, V. *Solid State Ionics* **1997**, *101−103*, 45.
(20) Michel, D.; Faudot, F.; Gaffet, E.; Mazerolles, L. *J. Am. Ceram. Soc.* **1993**, *76*, 2884.
(21) Esaka, T.; Takai, S.; Nishimura, N. *Denki Kagaku* **1996**, *64*, 1012.

10.1021/cm010770p CCC: $22.00 © 2002 American Chemical Society
Published on Web 05/02/2002

are called "mechanochemical reaction". It has been reported that the "mechanochemical reaction" could take place by a thermodynamically unfavorable route.[13−16] Therefore, we can expect to obtain new materials which could not be synthesized by a conventional melt-quenching method with a thermodynamical reaction. In addition, we can point out several advantages as a preparation procedure of amorphous solid electrolytes: this procedure is basically a room-temperature process[20,21] and useful for obtaining fine powders directly for solid lithium secondary batteries. Such fine powders improve interfacial contacts between an electrolyte and an electrode. The powders prepared by mechanical milling, thus, could also enhance battery performances.

We have prepared high lithium ion conducting amorphous materials in the system Li_2S-SiS_2 by mechanical milling.[22,23] Conductivities of these materials were 1.5×10^{-4} S cm^{-1} at room temperature; this value was comparable to that of powder glass prepared by melt quenching.[22] In addition, the materials exhibited high electrochemical stability at a wide potential of 10 V and the lithium ion transport number was almost unity. Furthermore, all solid-state cells with the amorphous materials as a solid electrolyte worked as a lithium secondary battery.[24]

In the present study we have synthesized lithium ion conducting materials in the system Li_3N-SiS_2 by mechanical milling at room temperature; Li_3N is used not only as a lithium source but also as a nitrogen source. Structure and properties as solid electrolytes of the obtained Li_3N-SiS_2 materials are investigated and they are compared with those of Li_2S-SiS_2 amorphous materials previously reported.[22,23] A formation process of the mechanically milled samples in the system Li_3N-SiS_2 is also discussed.

2. Experimental Section

Reagent-grade Li_3N (Aldrich; 99.9%, 80 mesh) and SiS_2 (Furuuchi Chem.; 99.9%) were used as starting materials. They were mixed at an appropriate mole ratio in an agate mortar beforehand. Compositions of starting materials were xLi$_3$N:(100−x)SiS$_2$ (x = 20, 30, 40, 50, and 60). Mechanical milling treatments were carried out for the starting materials using a planetary ball mill (Fritsch Pulverisette 7) with a rotation speed of ≈230 rpm at room temperature. Alumina was selected as pots and balls for planetary ball milling. The volume of pots, the diameter of balls, and the number of balls were 45 mL, 10 mm, and 10, respectively. Balls-to-mixture weight ratios ranged from 10:1 to 20:1. All of the treatments were carried out in a dry N_2-filled glovebox.

To identify crystalline phases of samples obtained by mechanical milling, X-ray diffraction measurements (shimadzu XRD-6000 diffractometer) were performed for powdered samples after mechanical milling for a given period. A surface of the samples was covered with a polyimide thin film for the protection of the samples from an attack of oxygen and moisture. In addition, local structures around silicon atoms were investigated by using solid-state ^{29}Si MAS NMR measurements (Valian Unity Inova 300 NMR spectrometer). The powdered samples were loaded into a zirconia sample tube with a sealant; these procedures were performed in a dry N_2-filled glovebox. Measurement conditions for ^{29}Si MAS NMR were as follows: the observed frequency was 59.59 MHz, the 90° pulse length was 1.5−2.5 μs, the recycle pulse delay was 30−180 s, the spinning speed was 3000−3500 Hz, the number of scans was 1000−8000, and reference standard was polydimethylsilane. Morphologies of mechanically milled samples were investigated by a scanning electron microscope (SEM) (JEOL Model JSM-5300).

Electrical conductivities were measured for pelletized samples, whose diameter and thickness were 10 mm and about 1 mm, respectively. The pelletized samples were obtained by cold-pressing under 3700 kg cm^{-2}. An ac impedance measurement was carried out for the pelletized samples, where carbon paste was painted as electrodes on both faces of the samples. The measurement was carried out in a dry Ar atmosphere using an impedance analyzer (Solartron, SI 1260) from 100 Hz to 15 MHz in the temperature range 30−220 °C. A dc conductivity was also measured using lithium plates as nonblocking electrodes and platinum plates as blocking electrodes to determine the lithium ion transport number of the mechanically milled samples. A cyclic voltammetry was carried out for the simple two-probe cell with a platinum plate as the working electrode and a lithium plate as the counter electrode. A scanning rate of 5 mV/s was used and this measurement was performed using a potentiostat (Hokuto Denko, HA-501) and a function generator (Hokuto Denko, HB-104).

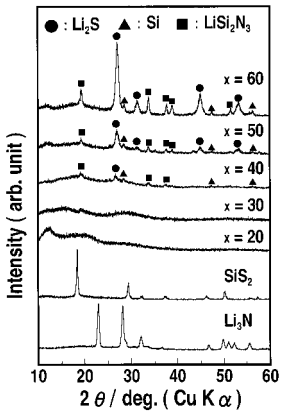

Figure 1. X-ray diffraction patterns of the xLi$_3$N:(100−x)-SiS$_2$ powder materials after mechanical milling for 20 h.

3. Results and Discussion

3.1. X-ray Diffraction. Figure 1 shows the X-ray diffraction patterns of powder samples with nominal compositions of xLi$_3$N:(100−x)SiS$_2$ (x = 20, 30, 40, 50, and 60) after mechanical milling for 20 h at room temperature. The diffraction patterns of starting materials of Li_3N and SiS_2 crystals are also shown in this figure. The samples at the composition of x = 20 and 30 show halo patterns with no diffraction peaks, suggesting that the mixture of the starting materials becomes amorphous by mechanical milling for 20 h. On the other hand, new diffraction peaks due to Li_2S, Si, and $LiSi_2N_3$ crystals are observed in the samples at the compositions of x = 40, 50, and 60. Those diffraction peaks did not change in the samples further mechanically milled over 20 h. The diffraction peaks become sharper with an increase in the Li_3N content. The formation of $LiSi_2N_3$ crystals in those mechanically milled samples suggests that nitrogen atoms are introduced into the obtained samples. Therefore, nitrogen atoms are also presumed to be in the amorphous phases of the samples at the compositions of x = 20 and 30.

3.2. Electrical Conductivity. Figure 2 shows the temperature dependence of electrical conductivities of

(22) Morimoto, H.; Yamashita, H.; Tatsumisago, M.; Minami, T. *J. Am. Ceram. Soc.* **1999**, *82*, 1352.
(23) Yamashita, H.; Hayashi, A.; Morimoto, H.; Tatsumisago, M.; Minami, T.; Miura, Y. *J. Ceram. Soc. Jpn.* **2000**, *108*, 973.
(24) Komiya, R.; Hayashi, A.; Morimoto, H.; Tatsumisago, M.; Minami, T. *Solid State Ionics* **2001**, *140*, 83.

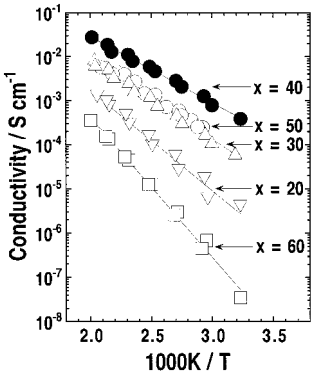

Figure 2. Temperature dependence of electrical conductivities of the xLi$_3$N:(100−x)SiS$_2$ pelletized materials after mechanical milling for 20 h.

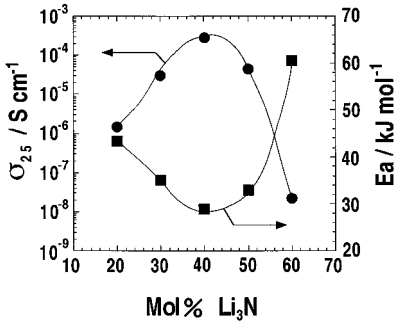

Figure 3. Conductivities at 25 °C (σ_{25}) and activation energies (E_a) for conduction of the xLi$_3$N:(100−x)SiS$_2$ materials after mechanical milling for 20 h.

the samples with nominal compositions of xLi$_3$N:(100−x)SiS$_2$ (x = 20, 30, 40, 50, and 60) after mechanical milling for 20 h. The conductivities of the mechanically milled samples follow the Arrhenius-type equation

$$\sigma = \sigma_0 \exp(-E_a/RT)$$

where E_a is the activation energy for conduction, σ_0 the pre-exponential factor, and R the gas constant. Composition dependences of conductivities at 25 °C (σ_{25}) and activation energies (E_a) are shown in Figure 3. The σ_{25} values of the materials increase up to x = 40 and then decrease with an increase in x. The σ_{25} exhibits a maximum value of 2.7 × 10^{-4} S cm^{-1} at the composition of x = 40. The composition dependence of E_a corresponds to that of σ_{25}; the E_a exhibits a minimum value of 29 kJ mol^{-1} at the composition of x = 40.

3.3. Structural Analysis. We have investigated a structure of amorphous phases by ^{29}Si MAS NMR measurements, which determine coordination states around silicon atoms. Figure 4 shows the ^{29}Si MAS NMR spectra of the samples with nominal compositions of xLi$_3$N:(100−x)SiS$_2$ (x = 20, 30, 40, 50, and 60) after mechanical milling for 20 h. The spectra of Si$_3$N$_4$ crystal and the 95(0.6Li$_2$S:0.4SiS$_2$):5Li$_4$SiO$_4$ oxysulfide glass prepared by melt quenching are also shown in this figure for comparison. Two peaks at around 5 and −3 ppm are observed in the sample at the composition of x = 20. In the samples at x = 30, 40, and 50, four broad peaks at around −25, −50, −55, and −80 ppm are newly observed besides the peaks at 5 and −3 ppm. In the sample at x = 60, the peak at around −80 ppm is only observed.

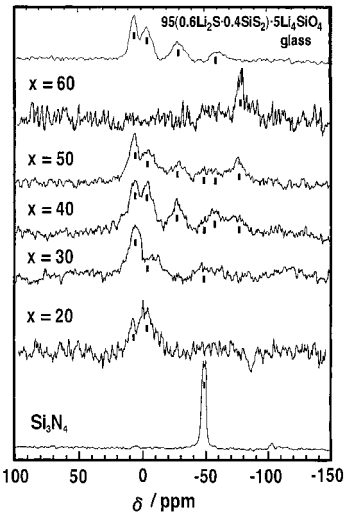

Figure 4. ^{29}Si MAS NMR spectra of the xLi$_3$N:(100−x)SiS$_2$ materials after mechanical milling for 20 h.

Two peaks at around 5 and −3 ppm are assigned to SiS$_4$ tetrahedral units; the peak at 5 ppm is due to the SiS$_4$ units with no edge-sharing (E(0)) units, while the peak at −3 ppm is due to the SiS$_4$ units with one edge-sharing (E(1)) unit.[25,26] The peak at −80 ppm is due to a silicon atom in a silicon (Si) crystal. The peaks at around −25, −50, and −55 ppm are possibly due to SiN$_n$S$_{4-n}$ (n = 1, 2, 3) tetrahedral units in which a silicon atom is coordinated with both nitrogen and sulfur atoms. On the other hand, the peak positions of −25 and −55 ppm are in good agreement with those observed in the oxysulfide glass as shown in Figure 4. Therefore, the peaks at −25 and −55 ppm are possibly due to SiO$_2$S$_2$ and SiO$_3$S tetrahedral units, respectively; the peak due to SiOS$_3$ units, which are also present in the oxysulfide glass, is overlapped by the peak at −3 ppm.[27] The peak at −50 ppm cannot be observed in the spectrum of the oxysulfide glass but this peak is observed in a silicon nitride (Si$_3$N$_4$) crystal, suggesting that the peak at −50 ppm must be due to silicon-centered units with some Si−N bonds.

It is found that amorphous phases of the samples in the system xLi$_3$N:(100−x)SiS$_2$ obtained by mechanical milling are mainly constructed by SiS$_4$ (E(0) and E(1)) units. The silicon-centered tetrahedral units with Si−N bonds are present in the samples at the composition $x \geq 30$; nitrogen atoms are introduced into an amorphous phase as well as a crystalline phase (LiSi$_2$N$_3$) since the sample at x = 30 is amorphous as shown in Figure 1. When the 40Li$_3$N:60SiS$_2$ sample was heated at 700 °C, the peak at −50 ppm due to the Si−N bond became intense, which also supports the presence of the Si−N bond in the amorphous phase. We tried to evaluate the nitrogen contents by using the Kjeldahl method. However, reproducible values of nitrogen contents have not been obtained, which is probably because of the inhibitory effect of the coexisting sulfur atoms.

The SiO$_n$S$_{4-n}$ (n = 1, 2, 3) units and Si units are partially present at the composition $x \geq 40$; oxygen

(25) Eckert, H.; Zhang, Z.; Kennedy, J. H. *J. Non-Cryst. Solids* **1989**, *107*, 271.
(26) Eckert, H.; Kennedy, J. H.; Pradel, A.; Ribes, M. *J. Non-Cryst. Solids* **1989**, *113*, 287.
(27) Hayashi, A.; Araki, R.; Tadanaga, K.; Tatsumisago, M.; Minami, T. *Phys. Chem. Glasses* **1999**, *40*, 140.

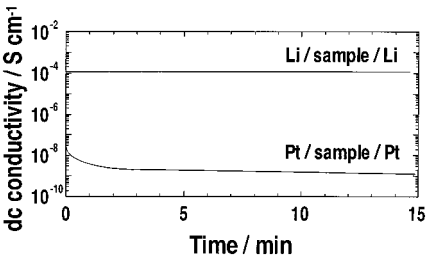

Figure 5. Time dependence of dc conductivities obtained from currents after applying a constant dc voltage of 1 V to the $40Li_3N{:}60SiS_2$ material after mechanical milling for 20 h.

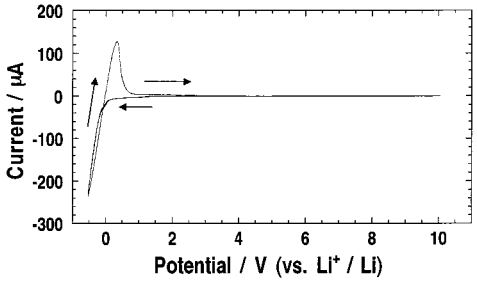

Figure 6. Cyclic voltammogram of the $40Li_3N{:}60SiS_2$ material after mechanical milling for 20 h.

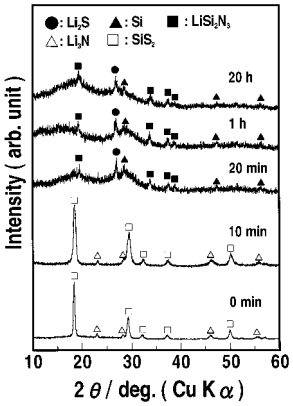

Figure 7. X-ray diffraction patterns of the $40Li_3N{:}60SiS_2$ materials obtained by different milling periods.

atoms in the former units are probably derived from oxide contaminations in the starting materials and from alumina of milling pots and balls during mechanical milling. The presence of Si units obtained by NMR measurements corresponds to the XRD results as shown in Figure 1; Si crystals were observed in the samples at the composition range $x \geq 40$.

We have confirmed that the high lithium ion conductive amorphous materials in the system Li_2S-SiS_2 are mainly constructed by E(0) units.[23] These structural units were also mainly present in the $xLi_3N{:}(100-x)$-SiS_2 materials at the composition range $30 \leq x \leq 50$. This similarity in local structure brought about high conductivities over 10^{-5} S cm^{-1} at room temperature as shown in Figure 3. The σ_{25} increased up to $x = 40$ and decreased with an increase in x. The increase in both SiS_4 units and lithium ion concentration brought about an increase in conductivities in the composition range $x \leq 40$, while the presence of a large amount of crystalline phase such as Li_2S (Figure 1) decreased conductivities of the samples in the range $x > 40$.

3.4. Lithium Ion Transport Number. The $40Li_3N{:}60SiS_2$ material mechanically milled for 20 h exhibited the highest conductivity of 2.7×10^{-4} S cm^{-1} at room temperature. However, it was revealed from XRD and NMR measurements that silicon crystals with an electronic conductivity were partially present in the material. To determine a lithium ion transport number of the material, a dc conductivity was measured using blocking and nonblocking electrodes. A constant dc voltage of 1 V was applied to the powder samples to obtain dc current−time curves. Figure 5 shows the dc conductivities at 25 °C as a function of time, which was derived from the dc current−time curves for the sample with the nominal composition of $40Li_3N{:}60SiS_2$. In the case of using lithium electrodes (nonblocking electrodes), a dc conductivity is almost constant with time; the conductivity value is around 1.0×10^{-4} S cm^{-1}, which almost agrees with the value obtained from ac impedance measurements using carbon electrodes (blocking electrodes) as shown in Figure 2. This result indicates that only lithium ion conduction occurs and the conduction of other ions is negligible in this material. In the case of using platinum plates (blocking electrodes), a large decrease of dc conductivities is initially observed and then the conductivity becomes almost constant. The conductivity value is about 4 orders of magnitude lower than the value obtained by using the lithium electrodes. This result suggests that an electronic conduction at total conductivity is almost negligible. It is revealed that the lithium ion transport number of the sample with the nominal composition of $40Li_3N{:}60SiS_2$ is almost unity, although small amounts of silicon crystals exist in the sample.

3.5. Electrochemical Property. We have determined the electrochemical window of the $40Li_3N{:}60SiS_2$ sample after mechanical milling for 20 h by cyclic voltammetry. Figure 6 shows the cyclic voltammogram of the $40Li_3N{:}60SiS_2$ sample. At first, a cathodic current due to a deposition of metallic lithium is observed on a cathodic sweep up to −0.5 V (vs Li^+/Li). Then, an anodic current due to a dissolution of metallic lithium is observed around +0.4 V on an anodic sweep. No anodic current peaks except for the peak due to lithium dissolution are observed up to +10 V. Thus, the $40Li_3N{:}60SiS_2$ sample has a very wide electrochemical window of about 10 V despite the sample including Li_3N as a starting material, which shows a very low decomposition voltage (0.445 V).

The $40Li_3N{:}60SiS_2$ material obtained by mechanical milling exhibits a high lithium ion conductivity, a single lithium ion conduction, and a wide electrochemical window. Therefore, this material is one of the most promising solid electrolytes for lithium ion secondary batteries.

3.6. Formation Process of the $40Li_3N{:}60SiS_2$ Ion Conducting Material by Mechanical Milling. We have investigated a formation process of the sample with a nominal composition of $40Li_3N{:}60SiS_2$ by mechanical milling. Figure 7 shows the X-ray diffraction patterns of the $40Li_3N{:}60SiS_2$ samples at different milling periods. Diffraction peaks due to Li_3N and SiS_2 crystals are observed in the sample without mechanical milling, which is just a mixture of the starting materials. After mechanical milling for 10 min, the peaks due to Li_3N and SiS_2 slightly broaden. After mechanical milling for 20 min, a XRD pattern is drastically changed;

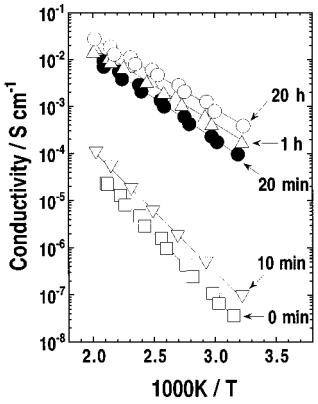

Figure 8. Temperature dependence of conductivities for the $40Li_3N:60SiS_2$ materials obtained by different milling times.

the peaks due to Li_3N and SiS_2 disappear, new peaks due to Li_2S, Si, and $LiSi_2N_3$ appear, and all of the diffraction peaks broaden. The diffraction pattern of the sample at 20 h is similar to that of the sample at 20 min. These results indicate that explosive mechanochemical reactions[28,29] between Li_3N and SiS_2 crystals instantaneously occurred during the first 20 min to form amorphous phases with some crystalline phases; an introduction of nitrogen atoms into the obtained sample occurs in this period. Crystallinity of Li_2S, Si, and $LiSi_2N_3$ no longer changes with further mechanical milling over 20 min.

Figure 8 shows the temperature dependence of electrical conductivities of the samples with the nominal composition of $40Li_3N:60SiS_2$ at different milling periods. A mixture without mechanical milling (0 min) has a conductivity around 10^{-8} S cm^{-1} at room temperature and an activation energy of 52 kJ mol^{-1}. The conductivities of the sample drastically increase after mechanical milling for 20 min; the conductivity is about 3 orders of magnitude higher than that of 10 min. The sample mechanically milled for 20 min exhibits a high conductivity around 10^{-4} S cm^{-1} at room temperature and an activation energy of 34 kJ mol^{-1}. After mechanical milling for 20 min, the conductivities of the sample gradually increase with an increase in the mechanical milling period.

The change of coordination states around silicon atoms due to the explosive reactions by mechanical milling has been investigated using NMR measurements. Figure 9 shows the ^{29}Si MAS NMR spectra of the samples with a nominal composition of $40Li_3N:60SiS_2$ at different milling periods. A sharp peak is observed at around −20 ppm in the samples obtained after mechanical milling for 0 and 10 min. The spectrum drastically changes after mechanical milling for 20 min; the peak at around −20 ppm disappears and two peaks at around 5 and −3 ppm appear. These two peaks are also mainly observed in the samples after mechanical milling for 1 and 20 h. Four broad peaks around −25, −50, −55, and −80 ppm appear in the sample after mechanical milling for 20 min and the intensity of these peaks become stronger in the sample after mechanical milling for 20 h.

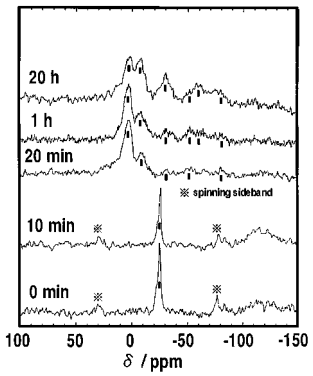

Figure 9. ^{29}Si MAS NMR spectra of the $40Li_3N:60SiS_2$ materials obtained by different milling times.

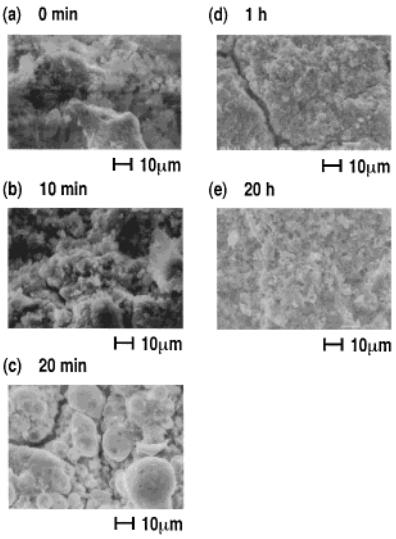

Figure 10. SEM photographs of a sectional view of the pellettized $40Li_3N:60SiS_2$ materials obtained by different milling times: (a) 0 min, (b) 10 min, (c) 20 min, (d) 1 h, and (e) 20 h.

The sharp peak at around −20 ppm is due to the SiS_4 tetrahedral units with two edge-sharing (E(2)) units;[30] this peak is observed in a SiS_2 crystal and the spectra for 0 and 10 min indicate the presence of SiS_2 crystals in those samples. Assignments of the peaks at 5, −3, −25, −50, −55, and −80 ppm have already been described in section 3.3.

The E(2) units disappear and E(1) and E(0) units newly appear after mechanical milling for 20 min, suggesting that the mechanical milling for 20 min introduces considerable strains and defects into the SiS_2 crystal structure and destroys the edge-shared bonds between SiS_4 tetrahedral units. Subsequently, the disordered SiS_2 reacts with Li_3N to form E(1) and E(0) and silicon units with Si−N bonds. The SiO_nS_{4-n} (n = 1, 2, 3) units gradually form in the periods during mechanical milling over 20 min.

Morphologies of those samples were investigated by a scanning electron microscope (SEM). Figure 10 shows the SEM photographs of the samples with the composition of $40Li_3N:60SiS_2$ at different milling periods (a)−(e). Each photograph shows a sectional view of the pelletized samples. In the sample milled for 10 min (b),

(28) Chakurov, C.; Rusanov, V. Koichev, J. *J. Solid State Chem.* **1987**, *71*, 522.
(29) Rusanov, V.; Chakurov, C. *J. Solid State Chem.* **1989**, *79*, 181.
(30) Tenhover, M.; Boyer, R. D.; Henderson, R. S.; Hammond, T. E.; Shreve, G. A. *Solid State Commun.* **1988**, *65*, 1517.

the morphology of the sample is similar to that of the as-mixed powder (a). The morphology of the sample drastically changes in the sample milled for 20 min (c); large spherical grains of about 10 μm in diameter are observed. With further mechanical milling over 20 min, the size of grains gradually decreases with an increase in the mechanical milling periods ((c)−(e)); particles of a few micrometers in diameter are mainly obtained in the sample milled for 20 h (e).

It is revealed from the results of XRD (Figure 7), NMR (Figure 9), and SEM (Figure 10) measurements that the local structure and particle morphology of the mechanically milled samples drastically change during the milling period between 10 and 20 min. Although, in general, mechanochemical reactions gradually proceed by solid-state interdiffusion reactions among powder mixtures, it is also reported that explosive reactions with partial melting of powders can occur during a mechanochemical synthesis; the latter reaction is especially called "a self-propagating combustive reaction".[28,29,31,32] The morphology of the samples mechanically milled for 20 min suggests that the explosive reactions occur in the samples.

The sample after mechanical milling for 20 min mainly consisted of E(0) units. As described in section 3.3, the amorphous phase mainly containing E(0) units exhibited high electrical conductivities. The conductivity drastically increased after mechanical milling for 20 min as shown in Figure 8 since large amounts of E(0) units formed in the mechanically milled samples for this period. The SEM photographs as shown in Figure 10 indicated that the size of the particles decreased and then close contact among particles could be achieved with an increase in milling periods over 20 min. Since the close contact of particles lowers grain-boundary resistances, the conductivity gradually increased with an increase in the milling periods as shown in Figure 8.

3.7. Comparison to the Li_2S-SiS_2 System. We have reported that electrical conductivities of the $60Li_2S:40SiS_2$ amorphous powder mechanically milled for 20 h are over 10^{-4} S cm^{-1} at room temperature.[22,23] This material also exhibited excellent properties as solid electrolytes such as unity of lithium ion transport number and a wide electrochemical window. The mechanically milled $40Li_3N:60SiS_2$ material obtained in the present study showed superior performance as solid electrolytes comparable to the mechanically milled $60Li_2S:40SiS_2$ materials. This is because local structures around silicon atoms of both materials are very similar; both materials mainly consist of E(0) units. ^{29}Si MAS NMR spectra of the $40Li_3N:60SiS_2$ material indicated that the structural units with Si−N bonds were also present in the glass structure as shown in Figure 4.

In the Li_2S-SiS_2 system, the mechanical milling treatment for 5 h with a rotation speed of 370 rpm was at least required to obtain materials with high conductivities more than 10^{-4} S cm^{-1} at room temperature.[23] On the other hand, the treatment for 20 min with a rotation speed of 230 rpm was required in the system Li_3N-SiS_2. Therefore, energies of mechanical milling required to obtain high conductive materials are considerably lower in the system Li_3N-SiS_2 than in Li_2S-SiS_2. The mechanochemical reaction gradually proceeded by solid-state interdiffusion reactions in the system Li_2S-SiS_2, while the reaction explosively proceeded by self-propagating combustive reactions in the system Li_3N-SiS_2.

4. Conclusions

Lithium ion conducting materials in the system Li_3N-SiS_2 were synthesized by mechanical milling using a high-energy ball-milling technique at room temperature. The obtained materials were mainly amorphous; the materials with large amounts of Li_3N partially included some crystalline phases such as Li_2S, Si, and $LiSi_2N_3$. The amorphous phases were mainly constructed by the SiS_4 units with no edge-sharing (E(0)) units, which were also mainly present in the mechanically milled Li_2S-SiS_2 amorphous materials. The highest conductivity at room temperature was 2.7×10^{-4} S cm^{-1} and the activation energy was 29 kJ mol^{-1} for the $40Li_3N:60SiS_2$ material mechanically milled for 20 h. The lithium ion transport number was almost unity and the materials exhibited high electrochemical stability in a wide potential range of 10 V vs Li^+/Li. The conductivities of $40Li_3N:60SiS_2$ drastically increased during the first 20 min of mechanical milling because the E(0) units formed in this period. The morphology of $40Li_3N:60SiS_2$ also drastically changed during this period, suggesting that explosive thermal reactions occurred by mechanical milling.

Acknowledgment. This work was supported by the Grant-in-Aid for Scientific Research on Priority Areas (B) and Section (B) from the Ministry of Education, Science, Sports, and Culture of Japan and by Research Fellowships of the Japan Society for the Promotion of Science for Young Scientists.

CM010770P

(31) Takacs, L. *Mater. Res. Soc. Symp. Proc.* **1993**, *286*, 413.
(32) Takacs, L.; Susol, M. A. *J. Solid State Chem.* **1996**, *121*, 399.